LANGMUIR Article
Cite This: Langmuir XXXX, XXX, XXX−XXX
pubs.acs.org/Langmuir

Droplet Imbibition Enables Nonequilibrium Interfacial Reactions in Charged Microdroplets

Taghi Sahraeian, Dmytro S. Kulyk, and Abraham K. Badu-Tawiah*

Department of Chemistry and Biochemistry, The Ohio State University, Columbus, Ohio 43210, United States

Supporting Information

ABSTRACT: A droplet imbibition experiment is proposed to study interfacial effects, which appears to be the main factor influencing reaction acceleration in charged microdroplets produced by electrospray ionization (ESI). One reagent is deposited onto the surface of rapidly moving microdroplets containing the second reagent to be reacted. In this manner, reactions are hindered from reaching equilibrium and monitored in real time by mass spectrometry. We demonstrated this phenomenon using Katritzky chemistry, which is known to proceed either by the solvent-stabilized 2*H*-pyran intermediate or via the surface-active pseudobase intermediate. Comparisons with reactions performed using ESI show obvious surface effects in favor of the droplet imbibition experiment. By keeping reactant mole ratio constant, it was demonstrated that similar interfacial effects observed in the droplet imbibition experiment can be reached by allowing ESI microdroplets containing premixed reagents to traverse a distance >16 mm. At such spray distance, molecular diffusion and droplet lifetime become comparable allowing reactants to be enriched at droplet surface. Reactions were also conducted in rapid mixing, theta capillary-based droplets, which showed markedly reduced yields compared with the interfacial droplet imbibition experiment.

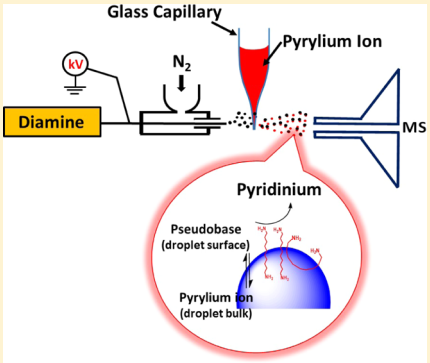

INTRODUCTION

Significant enhancements in reaction rates have been reported in confined (small) volume environments such as micelles,[1] emulsions,[2] nanocapsules,[3] microfluidic systems,[4] and more recently in charged microdroplets derived from electrospray ionization (ESI).[5−7] These experimental observations are important because they have direct implications in atmospheric/environmental[8,9] chemistry, origin of life,[10] and chemical synthesis.[11] In particular, air−water microlayers are ubiquitous from which aqueous droplets (aerosols) can be created; the lifetimes of these aerosols control chemical reactions and determine whether equilibrium can be reached or not. Limiting these reactions from reaching equilibrium can provide new insights into reaction pathways and, subsequently, determine the actual effects governing the rate enhancements observed in the droplet environment.

A multitude of empirical observations point to interfacial/surface effects as the main factor controlling reaction acceleration for bimolecular systems in confined volume.[12−17] In a specific experiment involving emulsion droplets, Fallah-Araghi et. al.[18] proposed that the residual unreacted carboxylate head groups, found in perfluoropolyether Krytox FS (MW: 7000−7500) surfactant, interacted with both the cationic reactants and product at the droplet interface. This surface adsorption was thought to be responsible for the ∼45-fold increase in the reaction rate compared with the corresponding reaction performed in the bulk solution. In an attempt to investigate the role of interfacial effects in reaction accelerations observed for charged microdroplets and in thin films, Li et. al.[19] utilized the known strong intermolecular hydrogen bond interaction between methyl and nitro functional groups. In this case, the interfacial adsorption of *p*-methylbenzaldehyde promoted by the presence of *p*-nitrobenzaldehyde allowed a 15-fold increase in the reaction rate for Claisen−Schmidt base-catalyzed condensation reactions performed in droplets and thin films at the ambient paper surface. The authors argued that neither evaporation of the solvent nor more effective mixing can explain the anomalous *p*-methylbenzaldehyde result, which was supported by the large difference in ρ-values between Hammett plots for thin-film-accelerated reaction and bulk-phase reaction. For reaction acceleration in charged microdroplets, surface effects can be caused not only by the concentration of reactants at the droplet surface but also by the sharp change in droplet pH. Protons at the charged droplet surface are deemed more acidic than normal Brønsted acids due to the absence of counterions. Such abundant charging of the microdroplets accompanied by high effective surface area was thought to be responsible for the observed 10^6 rate enhancement of Pomeranz−Fritsch synthesis.[20]

The chemically induced surface enrichment phenomenon is interesting as it can be made selective, but it is limited to near-equilibrium reactions. For charged microdroplet reactors, surface enrichment is inherent in the ESI process. For the

Received: August 5, 2019
Revised: October 17, 2019
Published: October 17, 2019

DOI: 10.1021/acs.langmuir.9b02439
Langmuir XXXX, XXX, XXX−XXX

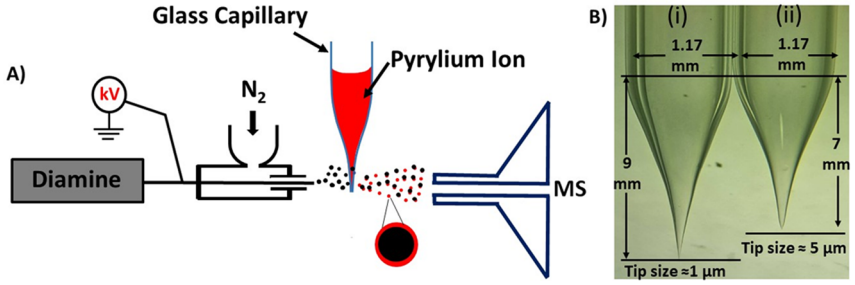

Figure 1. (A) Experimental setup for droplet imbibition where 1,12-dodecyl diamine-containing microdroplets are used to "pick-up" the pyrylium cation present in the glass capillary. Reaction products are, subsequently, detected by the mass spectrometer in real time. (B) Photograph showing a typical pulled glass capillary for (i) nanoelectrospray ionization (nESI) and (ii) droplet imbibition experiment.

generation of positively charged droplets, the intense electric field at the electrospray (ES) capillary tip draws some of the cations in the exposed solution to the liquid surface.[21−25] The electrohydrodynamics of the charged liquid surface causes the formation of Taylor cone from which a thin filament of the solution extends until it breaks up into droplets. Like the solution making up the Taylor cone, the droplets produced have a surface composition enriched in cations. Surface enrichment can be further promoted by allowing evaporation of droplets as they move in air toward a collector surface. These evaporating droplets are used in many cases where reaction acceleration is observed.[6] Droplet fusion or extractive electrospray experiments for rapid reactant mixing combined with evaporating droplets have also been shown to accelerate chemical reactions.[26−28] Herein, we describe a new droplet imbibition experiment that has the potential to effectively capture the structure and dynamics of reactant accumulation via nonequilibrium molecular adsorption onto the surface of rapidly moving microdroplets.

Assuming Brownian motion ($x^2 = 2Dt$, where x is the distance traveled, D is the diffusion coefficient, and t is the time), it will require milliseconds time scale for a small organic compound (e.g., fluorescein; aqueous diffusion coefficient is 0.64×10^{-9} m^2/s)[29] to traverse a 5 μm droplet. This suggests that a charged microdroplet moving at a typical speed of 100 m/s[26,30] across a <5 mm distance can be considered "frozen" in terms of surface activity/enrichment. The droplet lifetime (~50 μs) will be too short to allow further surface enrichment beyond that, which is set during Taylor cone formation. We used this apparent mismatch in droplet lifetime and molecular diffusion, at short distances, to study surface effects in the confined environment of the charged microdroplets. We demonstrate that the droplet pick-up process occurs with minimal mixing in the droplet imbibition platform; reactions conducted under this condition were observed to show markedly different reactivity when compared with evaporating droplets derived from electrospray and those generated from theta capillaries, which offer rapid mixing. Collectively, this study gives the first direct evidence that extricates interfacial effects in droplet chemistry from concentration effects derived from solvent evaporation.

MATERIALS AND METHODS

Droplet Imbibition Experimental Setup. The apparatus used for the imbibition experiment is shown in Figure 1A, which utilized a Swagelok union Tee element that allows two inputs: delivery of the spray solvent through the electrospray (ES) emitter on which a high direct current voltage is applied and nitrogen (N_2) nebulizer gas. Unless otherwise stated, the spray solvent consisted of MeOH/H_2O (1:1, v/v) in which one reagent (e.g., diamine) to be reacted is dissolved. The ES emitter comprises of a pair of inner (100 μm ID) fused silica (FS) capillary and outer (250 μm ID) FS capillary. The inner ES capillary is pushed through the Union Tee all the way to the outlet where it is adjusted to be slightly (~1 mm) outside of the outer capillary. The outer capillary allows the high-pressure N_2 gas to be delivered co-axially with the flow of the analyte solution, providing a fine mist of electrospray droplets. A pulled glass capillary (tip size ~5 μm, Figure 1B(ii)) containing the second reactant (e.g., pyrylium cation) is positioned between the ES emitter and mass spectrometer inlet. The distance between the ES emitter and the tip of the glass capillary and that between the tip of the glass capillary and the mass spectrometer inlet were kept at ~4 and 3 mm, respectively. In a typical experiment, the tip of the glass capillary is sampled by charged microdroplets derived from the ES emitter. As will be shown later, limited mixing occurs during the pick-up process, implying that chemical reactions between the diamine and the pyrylium occur at the droplet surface. This reaction is then monitored in real time by mass spectrometry (MS). Thermo Fisher Scientific linear ion trap mass spectrometer (San Jose, CA) was used. Optimized parameters for MS used were as follows: 5 kV spray voltage, 200 °C capillary temperature, 3 microscans, 100 ms ion injection time, and 60% S-lens voltage. MS data collecting and processing were executed using the Thermo Fisher Scientific Xcalibur 2.2 SP1 software. Tandem MS with collision-induced dissociation was utilized for the analyte identification.

Chemical and Reagents. 2,4,6-triphenylpyrylium tetrafluoroborate (98%), cortisone (98%), methanol (99.9% high-performance liquid chromatography (HPLC) grade), and acetonitrile (99.9% HPLC grade) were all obtained from Sigma-Aldrich (St. Louis). 1,12-diaminododecane (98%) and 1,3-diaminopropane were ordered from Fisher Scientific (Columbus, OH). Dodecylamine (98%) was ordered from Acros Organics (New Jersey). Ethanol (99.5%) was ordered from Decon Laboratories (King of Prussia, PA). All aqueous solutions were prepared in 18.2 MΩ water from a Milli-Q water purification system (Millipore, Billerica, MA).

RESULTS AND DISCUSSION

Selection of Chemical Systems. We used the Katritzky chemistry[31−34] involving the reaction between 2,4,6-triphenylpyrylium cation (**1**) and primary α, ω-diamines (carbon numbers, n = 3 and 12) as model systems. This reaction was selected because a recent study utilizing surface-enhanced Raman spectroscopy and MS showed the presence of two distinct intermediates depending on the level of reactant solvation:[34] bulk solution-phase reaction conditions favored a 2*H*-pyran intermediate, whereas reactions occurring in a solvent-free environment were determined to involve a pseudobase intermediate. We hypothesized that the formation of pseudobase intermediate will be favored if the charge microdroplet reaction system embodies substantial surface effects. To further enhance surface activity, we devised a

DOI: 10.1021/acs.langmuir.9b02439
Langmuir XXXX, XXX, XXX−XXX

droplet imbibition experiment to allow the deposition of pyrylium ions onto the surface of rapidly moving charged microdroplets; the pyrylium ions were contained in a glass capillary, which was, subsequently, placed between the ESI emitter and the inlet of the mass spectrometer, as already described in Figure 1A. The glass capillary was pulled to a wider tip (5 μm) and a shorter protruding edge (Figure 1B(ii)) to facilitate reagent pick-up (imbibe) by the charged microdroplets. Pyrylium ions desorption from the microtip occurred at ~1.5 nL/min flowrates (see Figure S1 for optimization of the setup).

The Katritzky reaction was examined in two ways: in one experiment, the diamine was ionized and delivered in charged microdroplets to the pyrylium ions present in the glass capillary. In the other experiment, the reagents were interchanged and the pyrylium ions were sprayed toward the diamines. The former experiment is discussed first. The interfacial Katritzky reaction occurring under our novel droplet imbibition experimental condition was compared to the conventional charged microdroplet reaction where the diamine was premixed with pyrylium ion in methanol/water (50/50 (v/v)) solution before electrospray. Chemical pathways leading to the main products/intermediates from the reaction of **1** with 1,12-dodecyl diamine (**2**) are illustrated in Scheme 1. The formation of the monopyridinium product (**6**) involves two competing intermediates: (1) the pseudobase intermediate (**3**, MW: 326) is formed via reaction of **1** with water and (2) the 2*H*-pyran intermediate (**4**, MW: 508) is formed by direct reaction of **1** with **2**. Reaction efficiency was estimated using the ratio (R) of ion intensity of the reaction product of interest to the intensity of the unreacted pyrylium cation, all detected in a specific mass spectrum.

Scheme 1. Proposed Reaction Pathways for Katritzky Chemistry Involving Pyrylium Cation (1) and 1,12-Dodecyl Diamine (2)[a]

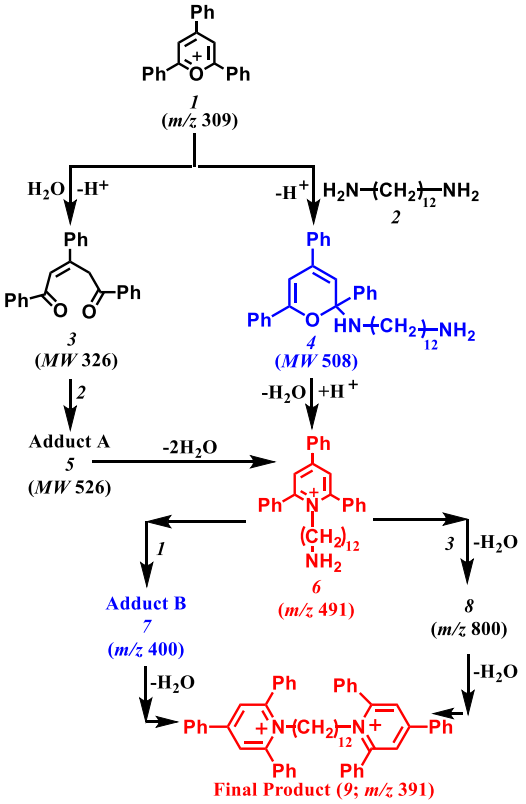

[a]The pseudobase intermediate (**3**) is favored at solvent-limited, interfacial conditions, while the 2*H*-pyran intermediate (**4**) is stabilized under bulk solution-phase conditions.

Comparison of Microdroplets and Bulk-Phase Reactivities. The 2*H*-pyran intermediate was detected at m/z 509 at the onset of the bulk solution reaction (Figure 2A) and

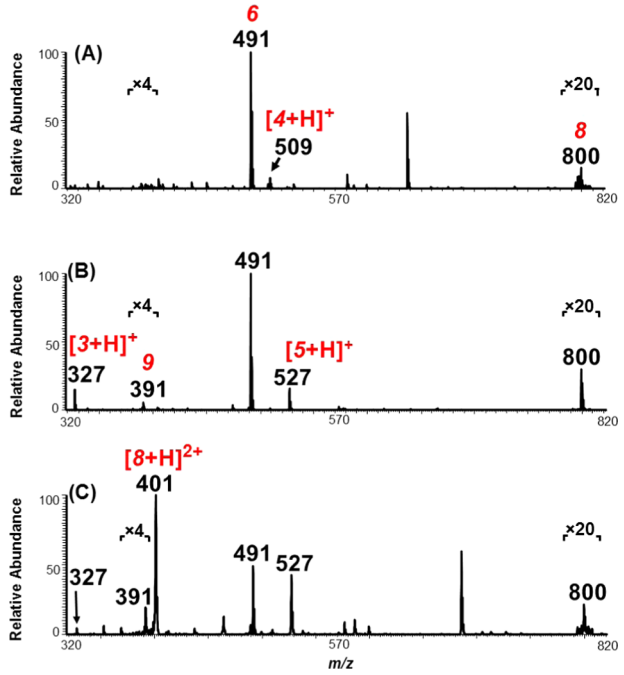

Figure 2. Positive-ion mode mass spectra showing reaction between 2,4,6-triphenylpyrylium cation and 1,12-dodecyl diamine using: (A) nESI-MS (bulk-phase reaction) at the onset of mixing the two reactants, (B) ESI-MS (conventional charged microdroplet reaction) at the onset of mixing the two reactants in the bulk solution phase, and (C) the droplet imbibition experimental setup. In all cases, reactants were prepared in methanol/water (1:1) solvent mixture.

the corresponding monopyridinium cation was formed at 5%, relative to the intensity of the unreacted pyrylium ion. The monopyridinium product is expected to react through two distinct intermediates (**7** and **8**) to give the dipyridinium product (**9**). No trace of product **9** was detected in the bulk-solution-phase reaction. The solution-phase reaction mixture was analyzed using nanoelectrospray ionization MS (nESI-MS), which produces less reactive nanodroplets.[35] Upon electrospray of the same solution, the resultant charged microdroplets showed markedly different product distributions, at the onset of mixing of the two reactants (Figure 2B). The monopyridinium and dipyridinium products were observed at 40 and 0.6% (relative to the abundance of **1**), respectively. This represents at least an 8-fold increase in reaction efficiency for monopyridinium production when compared with the bulk-phase reaction.

The uniqueness of the microdroplet reaction environment is exemplified by the type of intermediates involved. Unlike bulk-phase reaction where 2*H*-pyran intermediate was observed, we detected the pesudobase intermediate in the charged microdroplet experiment at m/z 327 and as adduct with **3** at m/z 527 (**5**, Adduct A). Also, there is no trace of Adduct B (**7**) at m/z 400 (i.e., the doubly charged adduct from **6** and **1**), which

DOI: 10.1021/acs.langmuir.9b02439
Langmuir XXXX, XXX, XXX−XXX

confirms the absence of the 2*H*-pyran intermediate and reinforcing interfacial effects in the ESI experiment. The precise mechanism of how the pseudobase intermediate is enriched at the surface of the charged microdroplet requires further investigations. However, this may be related to the time scale of the initial hydration reaction leading to **3**, which could be very efficient at the air−droplet interface. We anticipated that the separation of the pyrylium ion from the electrospray solvent and the deposition of it on the surface of the moving microdroplets should even enhance the formation and reactivity of the pseudobase intermediate. This expectation has been met.

Droplet Imbibition Reveals Droplets Dynamic and Structure. The resultant mass spectrum recorded after on-line exposure of diamine-containing microdroplets to **1** is provided in Figure 2C, which showed the formation of all expected products and intermediates related to pseudobase. The major difference is the appearance of the peak at m/z 401, which is the doubly charged species of intermediate **8**. The effective protonation of **8** under the droplet imbibition experiment signifies that this intermediate is formed near or at the surface, which, in turn, confirms the existence of the pseudobase at the droplet surface. The pseudobase itself and Adduct A were also detected at m/z 327 and 527, respectively. Like the conventional charged microdroplet reaction, no trace of the 2*H*-pyran intermediate (i.e., **4**, m/z 509 and Adduct B, m/z 400) was detected in the droplet imbibition experiment. This confirms our hypothesis that limited diffusion of reagent is to be expected given the short-time scales of the imbibition experiment. The fact that two molecules of diamine do not react with a single pseudobase molecule (containing two distinct carbonyl functional groups) indicates that the formation of Adduct A and the subsequent intramolecular ring closure via the loss of two water molecules (**5** → **6**, Scheme 1) to give the monopyridinium product (**6**, m/z 491) happen almost instantaneously.

Based on the above results on surface effects, two possible structures of diamine assembly at the droplet surface are proposed and illustrated in Scheme 2. That is, one or both of the amine functional groups in the diamine may be located at the air−droplet interface. If only one amine is found at the air−droplet interface (Scheme 2A), then we would expect the pyrylium ion to diffuse a minimum distance of ∼25 Å (the length of 1,12-dodecyl diamine) to encounter the second amine inserted inside the droplet. The intermediate corresponding to this event would occur at m/z 400, but it is not detected. Surprisingly, our results suggest that the U-shaped configuration, where both amines are exposed to air (Scheme 2B) is more probable due to the appearance of the m/z 401 species, which is possible only when the pseudobase (**3**) reacts with the free amine in **6**. The singly charged species of intermediate **8** is observed in all experiments at trace levels, but its charge state and exceedingly high abundance in the droplet imbibition setup indicate the presence of a unique condition, which we attribute to marked surface effects. We note that the peak at m/z 401 could correspond to the proton-bound dimer of the diamine. Although this peak is completely absent in conventional electrospray, even at high concentrations, tandem MS analysis (Figure S2) of control experiments suggests that its presence in the droplet imbibition experiment cannot be ruled out. We believe that the structure of assembly of the diamine at the droplet surface is dynamic, which can change from the straight packing (one amine at the interface) configuration into mixed packing mode where U-shape diamines present two free amines at the interface after the deposition of the pyrylium (Scheme 2B). In other words, the surface pyrylium species is able to trigger a response from the amine functional group where it moves from inside the droplet to the surface. Not only will this phenomenon facilitate interfacial reactions, but it will also increase the diamine evaporation rate from the droplet surface leading to high gas-phase concentration and a possible dimerization reaction.

Due to limited time and mixing, the final product **9** is trapped mainly as intermediate **8**. Ion intensities for Adduct A, **6**, **8**, and **9**, relative to that of **1**, were 10, 12, 24, and 0.4%, respectively. Although similar conversion ratios are seen for **9** in the two droplet-based reaction conditions, further experiments involving evaporative droplet (discussed later) have shown that the presence of doubly charged intermediate **8**, which is a primitive form of **9**, signifies > 10^3 times enhancement in reaction rate in favor of the droplet imbibition experiment.

Effect of Pyrylium Cation Concentration. The Katritzky reaction was also examined by reversing the reagents and electrospraying the pyrylium ion toward the diamine contained at the microtip glass capillary. Although this kind of droplet imbibition experiment was less efficient, we observed all possible intermediates, including the pseudobase, Adduct A, Adduct B, 2*H*-pyran, and intermediate **8** at m/z 327, 527, 400, 509, and 401, respectively (Figure 3A). This result is not surprising given that the initial electrosprayed droplets contain both the intact pyrylium (inside of droplet) and the pseudobase (at the surface of droplet), as well as the fact that the deposited diamine can respond and change orientation allowing access to inside of the droplet to react with intact pyrylium producing the doubly charged Adduct B. Clearly this situation is consistent with a nonequilibrium system that is able to access multiple reaction landscapes enabled by conformational changes at the droplet surface. The corresponding monopyridinium reaction product (**6**, m/z 491) was not stable; it released H_2 instantaneously to give species at m/z 489. The species at m/z 399 is formed from the complexation of ion at m/z 489 and **1** confirming our proposed mechanism in Scheme 1. Only a very small amount of **9** was observed at m/z 391. Note: in this droplet imbibition experiment, the electrosprayed pyrylium ion is in excess. Therefore, because of its high abundance, the pseudobase intermediate gave rise to many other new peaks (not shown), but proper structural

Scheme 2. Depiction of Droplet Structure and Reaction Dynamics Occurring in the Droplet Imbibition Experiment Leading to the Formation of Distinct Intermediates: (A) Striaght Packing Configuration where One Amine Reacts at the Droplet Surface and (B) Mixed Packing Configuraiton where a U-shaped Diamine Enables Both Amine Functional Groups to React at the Air−Droplet Interface

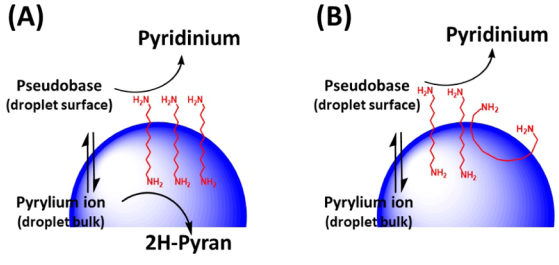

DOI: 10.1021/acs.langmuir.9b02439
Langmuir XXXX, XXX, XXX−XXX

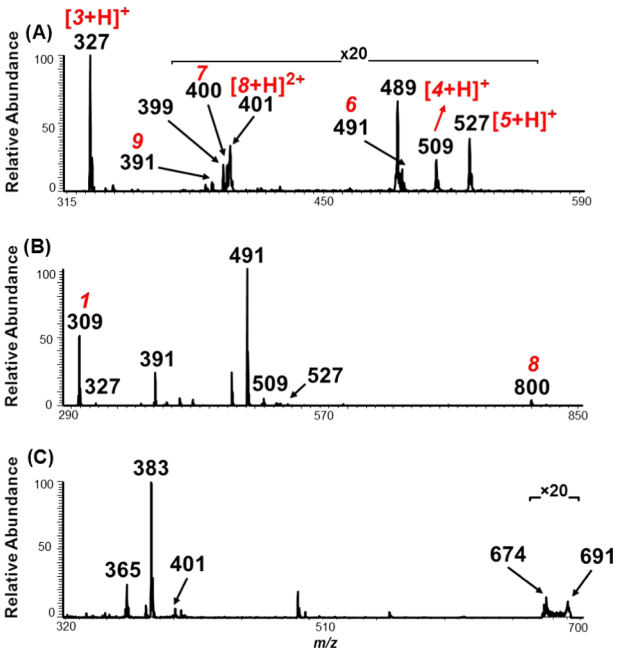

Figure 3. Mass spectra recorded using (A) droplet imbibition setup where 2,4,6-triphenylpyrylium cation was sprayed toward 1,12-dodecyl diamine contained in the glass capillary; (B) ESI-MS (conventional charged microdroplet reaction) when the reactant solution was prepared using 10× excess pyrylium ion and electrosprayed at the onset of mixing with 1,12-dodecyl diamine; (C) droplet imbibition setup where 1,3-diaminopropane was sprayed toward 2,4,6-triphenylpyrylium cation contained in the glass capillary. All reactants were prepared in methanol/water solvent mixture.

assignment would require further investigations due to the complexity of the reactions (perhaps because of the involvement of radical species indicated by the removal of hydrogen atoms). We investigated similar concentration effects in the bulk solution (methanol/water, 1:1) using 10× excess of the pyrylium ion. We observed a significantly reduced reaction efficiency, where no reaction products were detected even after 25 min of reaction time in bulk (Figure S3; analyzed with nESI-MS). Interestingly, when the same reaction mixture containing excess pyrylium ion was electrosprayed, we observed abundant ion signals for the monopyridinium and dipyridinium reaction products at 200% and 50%, relative to the signal from **1** (Figure 3B). This incredible rate acceleration supports the proposal that interfacial activities of reagents play crucial roles in reactions occurring in the charged microdroplet environment.

Droplet Reactivity Depends on Surface Activity of Reactants. The observed interfacial effect was further investigated by electrospraying a solution of 1,3-diaminopropane (MW 74), which has less surface affinity than **2**. As expected, exposure of **1** to 1,3-diaminopropane-containing microdroplets using our droplet imbibition experimental setup resulted in a much-reduced reaction efficiency compared to the corresponding reaction described above for **1** and **2**. The monopyridinium reaction product was observed at m/z 365 (0.5% relative to **1**; see Figure 3C) alongside the corresponding 2*H*-pyran and pseudobase intermediates at m/z 383 and 401, respectively (Figure 3C). The dipyridinium cation was not observed, but it appeared to have been trapped as two adducts of monopyridinium cation with **1** and **3**, which were detected at m/z 674 and 691, respectively. In addition to 1,3-diaminopropane being less surface active, the short carbon chain may also introduce a strong coulombic repulsion in the dipyridinium product due to the two adjacent positive charges. The short dwell time in our droplet imbibition experiment is also a contributing factor for the low yields and incomplete reactions observed.

Concentration Effects due to Evaporating Droplets. It was surprising that the conventional charged microdroplets from ESI did not register the presence of the doubly charged species of intermediate **8** (m/z 401) when the reagents were premixed. Surface enrichment in microdroplet reactivity can be enhanced via solvent evaporation. To investigate this effect, we performed the charged microdroplet reaction using different spray distances (2, 8, 16, and 24 mm) from the ESI emitter to the inlet of the mass spectrometer. To be completely consistent with the droplet imbibition experiment, the reaction mixture consisted of excess diamine (10×). The effect of each spray distance on the formation of m/z 401 ions was monitored at the onset of mixing of the two reactants. The results of this experiment are summarized in Figure S4, which showed increased amounts of m/z 401 species when the spray distance was increased. At 24 mm spray distance, the droplet lifetime is on the order of milliseconds time scale, which is comparable to molecular diffusion enabling significant concentration and surface effects. Concentration effect, due to reduced droplet volume, is seen in the concomitant appearance of the solution-phase 2*H*-pyran intermediate at m/z 509. The abundance of the Adduct A (m/z 527) also increased with spray distance signifying a more surface activity as the solvent evaporated. The corresponding bulk-phase reaction was also examined using nESI-MS at different reaction times. Here, m/z 401 appeared after 10 min (Figure S5). This will represent 10^8 times enhancement in reaction efficiency for the droplet imbibition experiment, which achieves comparable yields of m/z 401 in a matter of microseconds. The marked difference in appearance times for m/z 401 species in the three reaction systems (i.e., minutes for bulk phase, milliseconds for conventional ESI charged microdroplets, and microseconds for the droplet imbibition experiment) may signify major differences in diffusion rates[36] for species in the solution versus those inside of a charged microdroplet versus species at the surface of the charged microdroplet. Such a rapid diffusion rate at the curved droplet surface could account (among other factors) for the remarkable rate enhancements observed. The uniqueness of the droplet system includes new reaction pathways not available in the solution.[37] Such reaction is observed in the loss of H_2 from the monopyridinium cation, which occurred only in droplet-based reactions (Figures 3A and S5).

Effect of Mixing. The possible influence of mixing on the observed rate enhancement was investigated using theta capillary, which allowed the pyrylium cation and **2** to be sprayed from two separate chambers. Prior studies have shown mixing in theta capillaries to be completed within the microsecond lifetime of the droplets,[38−40] suggesting equilibrium type products should be formed under this theta capillary electrospray reaction condition. The mass spectrum recorded from the theta capillary spray experiment using excess pyrylium (10×) is provided in Figure S6, which showed no major product formation except the pseudobase intermediate and Adduct A at m/z 327 and 527, respectively. The absence of mono- and dipyrydinium reaction products is not surprising given that mixing in theta capillaries begins in the Taylor

DOI: 10.1021/acs.langmuir.9b02439
Langmuir XXXX, XXX, XXX−XXX

cone,[38] which resembles bulk mixing rather than interfacial effect. Further evidence of limited mixing in our droplet imbibition experiment is found in the fact that cortisone (100 μM), a hydrophilic, low-proton-affinity analyte (PA 787.8 kJ/mol)[41] showed comparable ion intensity as the surface-active dodecylamine analyte (100 μM; PA 879.5 kJ/mol)[42] (Figure S7B. Comparable ion intensities are observed after pick-up because cortisone remained distributed on the outside of the droplet, eliminating unfavorable competition for space. Marked difference in ion yields was observed when the two analytes were premixed in the solution before ESI (Figure S7A) signifying that cortisone was greatly suppressed by the surface-active dodecylamine analyte.

To further explore the possibility of mixing via convection during collision events in the droplet imbibition experiment, the reactants were prepared in two immiscible solvents: **1** was prepared in water and **2** in ethyl acetate. Although we do not expect mixing, the mono- and dipyrydinium products were detected at m/z 491 and 391 (trace), respectively, upon spraying the diamine organic solution toward the aqueous pyrylium cation (Figure 4). Two new peaks were observed at

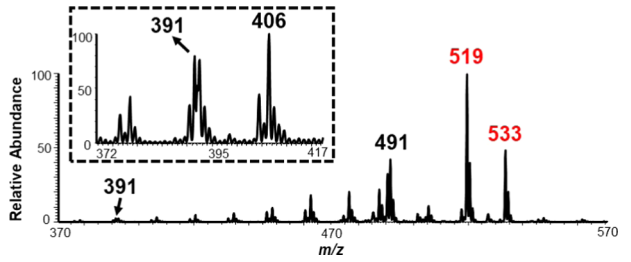

Figure 4. Positive-ion mode mass spectrum recorded from the droplet imbibition experiment when 1,12-dodecyl diamine in ethyl acetate organic solvent is sprayed toward the aqueous solution pyrylium cation solution present in the glass capillary. The insert shows the zoomed-in spectrum in m/z 370–417 range indicating the absence of doubly charged intermediate **8** at m/z 401.

m/z 519 and 533, which were identified in tandem MS experiments (Figure S8) as being related to **6**, formed via the reaction of the free amine in **6** with ethyl acetate solvent culminating in the addition of ethyl (MW: 29 Da) and acyl (MW: 43 Da) groups, respectively. The presence of these solvent-related species appears to have suppressed the formation of species at m/z 401 (see insert, Figure 4 for details). The solvent mismatch should prevent the pyrylium cation from diffusing into the ethyl acetate microdroplet. Therefore, the presence of the dipyridinium product is consistent with the proposed mechanism in Scheme 2B, where the diamine molecules are inserted in the microdroplet in a U-shaped fashion (anchored by the nonpolar hydrocarbon portion) where both of the polar amine groups are located at the air–droplet interface to allow the reaction with two molecules of pyrylium cations. This result, and those from the theta capillary experiments point toward interfacial effects, and that reagent mixing might contribute very little to the observed rate enhancements in the droplet imbibition experiment.

CONCLUSIONS

In summary, we have shown a simple but effective droplet imbibition approach to manipulate the surface of rapidly moving charged microdroplets to allow chemical reactions occurring at air–liquid interfaces to be examined in real time using MS. By employing the Katritzky pyrylium reaction with diamines, direct evidence for surface effects was obtained by detecting intermediates that are stabilized under solvent-limited conditions. Concentration effects resulting from solvent evaporation also play a role in reaction acceleration as seen in the reduction of the amount of time required for the monopyridinium cation to encounter the pyrylium ion for the charged microdroplet system (milliseconds) versus bulk solution-phase conditions (minutes). This study suggests that the droplet imbibition experiment can be used to screen various factors controlling confined volume reactions. The results also revealed that rapid mixing in confined microreactors could be important, but chemical reactions may still be limited if opportunities (e.g., evaporation, physical deposition, chemical stimulation, etc.) for surface enrichment are not created. Aside from rapid mixing and interfacial effects, droplet size can also influence results and deserves further investigation.

ASSOCIATED CONTENT

Supporting Information

The Supporting Information is available free of charge on the ACS Publications website at DOI: 10.1021/acs.langmuir.9b02439.

Experimental details and optimization of the droplet imbibition set-up; characterization of different reaction intermediates and products via collision-induced dissociation; bulk solution reaction of 1,12-dodecyl diamine and 10× excess pyrylium ion; effect of different spray distances on product and intermediate formation in traditional ESI; effect of bulk-phase reaction time on product and intermediate formation; theta capillary spray experiments for pyrylium ion and 1,12-dodecyl diamine reaction; comparison of ion suppression effect between conventional ESI and droplet imbibition; characterization of intermediates/dimervia collision-induced dissociation (PDF)

AUTHOR INFORMATION

Corresponding Author

*E-mail: badu-tawiah.1@osu.edu. Tel: 614-292-4276. Fax: (614) 292-1685.

ORCID

Abraham K. Badu-Tawiah: 0000-0001-8642-3431

Notes

The authors declare no competing financial interest.

ACKNOWLEDGMENTS

This research was supported by the U.S. Department of Energy, Office of Science, Office of Basic Energy Sciences, Condensed Phase and Interfacial Molecular Science, under award number DE-SC0016044.

REFERENCES

(1) Dwars, T.; Paetzold, E.; Oehme, G. Reactions in micellar systems. *Angew. Chem., Int. Ed.* **2005**, *44*, 7174–7179.

(2) Piradashvili, K.; Alexandrino, E. M.; Wurm, F. R.; Landfester, K. Reactions and Polymerizations at the Liquid–Liquid Interface. *Chem. Rev.* **2016**, *116*, 2141–2169.

(3) Taheri, S.; Baier, G.; Majewski, P.; Barton, M.; Forch, R.; Landfester, K.; Vasilev, K. Synthesis and antibacterial properties of a

DOI: 10.1021/acs.langmuir.9b02439
Langmuir XXXX, XXX, XXX–XXX

hybrid of silver−potato starch nanocapsules by miniemulsion/polyaddition polymerization. *J. Mater. Chem. B* **2014**, *2*, 1838−1845.
(4) Olivier, N.; Toupy, T.; Hartkoorn, R. C.; Desmet, R.; Monbaliu, J.-C. M.; Melnyk, O. Accelerated microfluidic native chemical ligation at difficult amino acids toward cyclic peptides. *Nat. Commun.* **2018**, *9*, No. 2847.
(5) Guardingo, M.; Busque, F.; Ruiz-Molina, D. Reactions in ultrasmall droplets by tip-assisted chemistry. *Chem. Commun.* **2016**, *52*, 11617−11626.
(6) Yan, X.; Bain, R. M.; Cooks, R. G. Organic Reactions in Microdroplets: Reaction Acceleration Revealed by Mass Spectrometry. *Angew. Chem., Int. Ed.* **2016**, *55*, 12960−12972.
(7) Kulyk, D. S.; Miller, C. F.; Badu-Tawiah, A. K. Reactive Charged Droplets for Reduction of Matrix Effects in Electrospray Ionization Mass Spectrometry. *Anal. Chem.* **2015**, *87*, 10988−10994.
(8) Cheng, Y.; Zheng, G.; Wei, C.; Mu, Q.; Zheng, B.; Wang, Z.; Gao, M.; Zhang, Q.; He, K.; Carmichael, G.; Pöschl, U.; Su, H. Reactive nitrogen chemistry in aerosol water as a source of sulfate during haze events in China. *Sci. Adv.* **2016**, *2*, No. e1601530.
(9) Küchler, A.; Yoshimoto, M.; Luginbühl, S.; Mavelli, F.; Walde, P. Enzymatic reactions in confined environments. *Nat. Nanotechnol.* **2016**, *11*, 409−420.
(10) Zwicker, D.; Seyboldt, R.; Weber, C. A.; Hyman, A. A.; Jülicher, F. Growth and division of active droplets provides a model for protocells. *Nat. Phys.* **2017**, *13*, 408−413.
(11) Bawazer, L. A.; McNally, C. S.; Empson, C. J.; Marchant, W. J.; Comyn, T. P.; Niu, X.; Cho, S.; McPherson, M. J.; Binks, B. P.; deMello, A.; Meldrum, F. C. Combinatorial microfluidic droplet engineering for biomimetic material synthesis. *Sci. Adv.* **2016**, *2*, No. 1600567.
(12) Girod, M.; Moyano, E.; Campbell, D. I.; Cooks, R. G. Accelerated bimolecular reactions in microdroplets studied by desorption electrospray ionization mass spectrometry. *Chem. Sci.* **2011**, *2*, 501−510.
(13) Banerjee, S.; Gnanamani, E.; Yan, X.; Zare, R. N. Can all bulk-phase reactions be accelerated in microdroplets? *Analyst* **2017**, *142*, 1399−1402.
(14) Bain, R. M.; Sathyamoorthi, S.; Zare, R. N. "On-Droplet" Chemistry: The Cycloaddition of Diethyl Azodicarboxylate and Quadricyclane. *Angew. Chem., Int. Ed.* **2017**, *56*, 15083−15087.
(15) Bain, R. M.; Pulliam, C. J.; Thery, F.; Cooks, R. G. Accelerated Chemical Reactions and Organic Synthesis in Leidenfrost Droplets. *Angew. Chem., Int. Ed.* **2016**, *55*, 10478−10482.
(16) Badu-Tawiah, A. K.; Campbell, D. I.; Cooks, R. G. Accelerated C−N Bond Formation in Dropcast Thin Films on Ambient Surfaces. *J. Am. Soc. Mass Spectrom.* **2012**, *23*, 1461−1468.
(17) Badu-Tawiah, A. K.; Campbell, D. I.; Cooks, R. G. Reactions of Microsolvated Organic Compounds at Ambient Surfaces: Droplet Velocity, Charge State, and Solvent Effects. *J. Am. Soc. Mass Spectrom.* **2012**, *23*, 1077−1084.
(18) Fallah-Araghi, A.; Meguellati, K.; Baret, J.-C.; Harrak, A. E.; Mangeat, T.; Karplus, M.; Ladame, S.; Marques, C. M.; Griffiths, A. D. Enhanced Chemical Synthesis at Soft Interfaces: A Universal Reaction-Adsorption Mechanism in Microcompartments. *Phys. Rev. Lett.* **2014**, *112*, 028301−028305.
(19) Li, Y.; Yan, X.; Cooks, R. G. The Role of the Interface in Thin Film and Droplet Accelerated Reactions Studied by Competitive Substituent Effects. *Angew. Chem., Int. Ed.* **2016**, *55*, 3433−3437.
(20) Banerjee, S.; Zare, R. N. Syntheses of Isoquinoline and Substituted Quinolines in Charged Microdroplets. *Angew. Chem., Int. Ed.* **2015**, *54*, 14795−14799.
(21) Konermann, L.; Ahadi, E.; Rodriguez, A. D.; Vahidi, S. Unraveling the Mechanism of Electrospray Ionization. *Anal. Chem.* **2013**, *85*, 2−9.
(22) Cech, N. B.; Enke, C. G. Practical implications of some recent studies in electrospray ionization fundamentals. *Mass Spectrom. Rev.* **2001**, *20*, 362−387.
(23) Miller, C. F.; Kulyk, D. S.; Kim, J. W.; Badu-Tawiah, A. K. Reconfigurable, multi-mode contained-electrospray ionization for protein folding and unfolding on the millisecond time scale. *Analyst* **2017**, *142*, 2152−2160.
(24) Kulyk, D. S.; Swiner, D. J.; Sahraeian, T.; Badu-Tawiah, A. K. Direct mass spectrometry analysis of complex mixtures by nano-electrospray with simultaneous atmospheric pressure chemical ionization and electrophoretic separation capabilities. *Anal. Chem.* **2019**, *91*, 11562−11568.
(25) Kulyk, D. S.; Sahraeian, T.; Wan, Q.; Badu-Tawiah, A. K. Reactive olfaction ambient mass spectrometry. *Anal. Chem.* **2019**, *91*, 6790−6799.
(26) Lee, J. K.; Kim, S.; Nam, H. G.; Zare, R. N. Microdroplet fusion mass spectrometry for fast reaction kinetics. *Proc. Natl. Acad. Sci. U.S.A.* **2015**, *112*, 3898−3903.
(27) Chen, H.; Venter, A.; Cooks, R. G. Extractive electrospray ionization for direct analysis of undiluted urine, milk and other complex mixtures without sample preparation. *Chem. Commun.* **2006**, 2042−2044.
(28) Nam, I.; Lee, J. K.; Nam, H. G.; Zare, R. N. Abiotic production of sugar phosphates and uridine ribonucleoside in aqueous microdroplets. *Proc. Natl. Acad. Sci. U.S.A.* **2017**, *114*, 12396−12400.
(29) Chiu, D. T.; Lorenz, R. M.; Jeffries, G. D. M. Droplets for Ultrasmall-Volume Analysis. *Anal. Chem.* **2009**, *81*, 5111−5118.
(30) Venter, A.; Sojka, P. E.; Cooks, R. G. Droplet Dynamics and Ionization Mechanisms in Desorption Electrospray Ionization Mass Spectrometry. *Anal. Chem.* **2006**, *78*, 8549−8555.
(31) Katritzky, A. R.; Marson, C. M. Pyrylium Mediated Transformations of Primary Amino Groups into Other Functional Groups. New Synthetic Methods. *Angew. Chem., Int. Ed.* **1984**, *23*, 420−429.
(32) Pyschev, A. I.; Krasnikov, V. V.; Zibert, A. E.; Tosyniyan, D. E.; Verin, S. V. New methodology for the conversion of pyrylium salts into pyridinium derivatives. *Mendeleev Commun.* **1996**, *6*, 99−101.
(33) Badu-Tawiah, A. K.; Wu, C.; Cooks, R. G. Ambient Ion Soft Landing. *Anal. Chem.* **2011**, *83*, 2648−2654.
(34) Badu-Tawiah, A. K.; Cyriac, J.; Cooks, R. G. Reactions of Organic Ions at Ambient Surfaces in a Solvent-Free Environment. *J. Am. Soc. Mass Spectrom.* **2012**, *23*, 842−849.
(35) Mortensen, D. N.; Williams, E. R. Ultrafast (1 μs) Mixing and Fast Protein Folding in Nanodrops Monitored by Mass Spectrometry. *J. Am. Chem. Soc.* **2016**, *138*, 3453−3460.
(36) Wang, H.; Fischman, G. S. Role of liquid droplet surface diffusion in the vapor-liquid-solid whisker growth mechanism. *J. Appl. Phys.* **1994**, *76*, 1557−1562.
(37) Müller, T.; Badu-Tawiah, A. K.; Cooks, R. G. Accelerated Carbon——Carbon Bond-Forming Reactions in Preparative Electrospray. *Angew. Chem., Int. Ed.* **2012**, *51*, 11832−11835.
(38) Mortensen, D. N.; Williams, E. R. Theta-Glass Capillaries in Electrospray Ionization: Rapid Mixing and Short Droplet Lifetimes. *Anal. Chem.* **2014**, *86*, 9315−9321.
(39) Fisher, C. M.; Kharlamova, A.; McLuckey, S. A. Affecting Protein Charge State Distributions in Nano-Electrospray Ionization via In-Spray Solution Mixing Using Theta Capillaries. *Anal. Chem.* **2014**, *86*, 4581−4588.
(40) Radionova, A.; Greenwood, D. R.; Willmott, G. R.; Derrick, P. J. Dual Nano-Electrospray and Mixing in the Taylor Cone. *Mass Spectrom. Lett.* **2016**, *7*, 21−25.
(41) Ma, Y.-C.; Kim, H.-Y. Determination of steroids by liquid chromatography/mass spectrometry. *J. Am. Soc. Mass Spectrom.* **1997**, *8*, 1010−1020.
(42) Gross, D. S.; Rodriguez-Cruz, S. E.; Bock, S.; Williams, E. R. Measurement of Coulomb Energy and Dielectric Polarizability of Gas-Phase Diprotonated Diaminoalkanes. *J. Phys. Chem. A.* **1995**, *99*, 4034−4038.

DOI: 10.1021/acs.langmuir.9b02439
Langmuir XXXX, XXX, XXX−XXX